

# Nanoscale investigations of shift of individual interfaces in temperature induced processes of Ni–Si system by secondary neutral mass spectrometry

A. Lakatos,<sup>1</sup> G. A. Langer,<sup>1</sup> A. Csik,<sup>2</sup> C. Cserhati,<sup>1</sup> M. Kis-Varga,<sup>2</sup> L. Daroczi,<sup>1</sup> G. L. Katona,<sup>1</sup> Z. Erdélyi,<sup>1</sup> G. Erdelyi,<sup>1</sup> K. Vad,<sup>2</sup> and D. L. Beke<sup>1,a)</sup>

<sup>1</sup>Department of Solid State Physics, University of Debrecen, H-4010 Debrecen P.O. Box 2, Hungary

<sup>2</sup>Institute of Nuclear Research, Hungarian Academy of Sciences (ATOMKI), H-4001 Debrecen P.O. Box 51, Hungary

(Received 2 September 2010; accepted 15 November 2010; published online 6 December 2010)

We describe a method for measurement of nanoscale shift of interfaces in layered systems by a combination of secondary neutral mass spectrometry and profilometer. We demonstrate it by the example of the investigation of interface shifts during the solid state reaction in Ni/amorphous-Si system. The kinetics of the shrinkage of the initial nanocrystalline Ni film and the amorphous Si layer as well as the average growth kinetics of the product phases were determined at 503 K. The results show that nanoscale resolution can be reached and the method is promising for following solid state reactions in different thin film systems. © 2010 American Institute of Physics. [doi:10.1063/1.3524491]

Determination of kinetics of motion of individual interfaces in nanotechnological processes requires high resolution techniques. For instance, in electronic devices a proper control of the growth of a few nanometer thick metal-silicide layers as interconnects is required. Most of the techniques and theoretical models for the investigation of the kinetics of such solid state reactions are usually restricted to the determination of the growth kinetics of the product phase, which is always a result of the simultaneous shift of *two interfaces* bordering the given phase. For example in case of a linear-parabolic growth<sup>1,2</sup> the values of the interface reaction rate coefficient  $K$  as well as the diffusion coefficient for the phase growth are effective values given by parameters belonging to the shift of both interface shifts: e.g., the effective interface reaction control parameter is given as  $1/K_{\text{eff}} = 1/K_1 + 1/K_2$ ,<sup>1</sup> where  $K_1$  and  $K_2$  are the corresponding parameters for the individual interfaces, respectively. Thus, for a deeper understanding, the knowledge of the kinetic parameters of *individual interface shifts* (and thus the experimental methods of their determination) is required. Knowing these one can easily compose their combination for the interpretation of the kinetics of phases. This is even so in nanoscale solid state reactions.<sup>2–6</sup> Indeed, it was shown that the linear kinetics for silicide formation is rather scarce on the micrometer scale,<sup>4</sup> while on nanoscale either a linear or a mixed linear-parabolic growth can be observed.<sup>2,6</sup> It was shown also theoretically (see, e.g., Ref. 5 and citations therein) that during interdiffusion between materials, in which the diffusion coefficients are orders of magnitude different (strong diffusion asymmetry), the interface shift on nanoscale can be anomalous and the kinetics can be linear even if there is no any extra potential barrier—corresponding to an interface reaction control—present.

One of the most promising techniques for determination of kinetics of solid state reactions on the nanoscale is the secondary neutral mass spectrometry (SNMS) by which

composition profiles can be constructed. While, for example x-ray diffraction (XRD) and differential scanning calorimetric techniques can only give information about the changes of the amount of the crystalline parent and product phase(s), SNMS technique can provide the positions of all individual interfaces present. However, in SNMS investigations the conversion of bombardment time of primary ion dose into eroded depth is a fundamental problem. Thus for the calculations of the composition-depth profiles the knowledge of both the sputtering yield and the density of the sample is needed.<sup>7,8</sup> In multilayers or in layered systems containing reaction (product) phases the sputtering yield and the density vary in general. As a consequence the sputter erosion rate is time dependent. The time dependence may cause serious difficulties in the accurate calibration of the eroded depth scale. This is so even if the depth scale of the SNMS profiles is calibrated by measuring the depth of the crater etched.

In this communication, we present a method in which we concentrate rather on the precise determination of the position of the interfaces than on the construction of well calibrated composition-depth profiles. The method is demonstrated in an initially nanocrystalline-Ni/amorphous-Si thin film system, in which during the solid state reaction new  $\text{Ni}_x\text{Si}_{1-x}$  phase(s) grow.

The 50 nm Ni/150 nm a-Si films were deposited onto (111) oriented *p*-type silicon and polycrystalline  $\text{Al}_2\text{O}_3$  substrates by dc magnetron sputtering at room temperature. The base pressure of the sputtering chamber was lower than  $2 \times 10^{-5}$  Pa. Circular Ni, Si, targets, 2 in. diameter were used. During the deposition of silicon and nickel layers the Ar (99.999%) pressure (under dynamic flow) and the sputtering power were  $5 \times 10^{-1}$  Pa and 40 W, as well as 1.2 Pa and 100 W, respectively. The deposition rates were calculated from the layer thickness measured by an AMBIOS XP-1 profilometer. The samples were annealed in vacuum (under  $10^{-4}$  Pa) and the sheet resistance of samples was measured *in situ* during the vacuum annealing by a four point technique. Symmetrical scans between  $40^\circ$  and  $60^\circ$  of the scat-

<sup>a)</sup>Electronic mail: dlbeke@tigris.klte.hu.

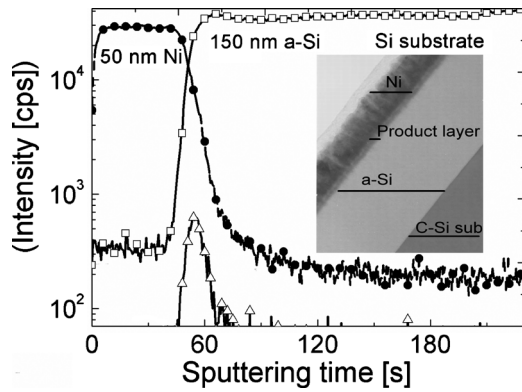


FIG. 1. Intensity-sputtering time curves of the as-deposited sample [■ -Ni, □ -Si, △-NiSi(1:1)]. The inset shows the TEM picture.

tering angle  $2\theta$  were performed by using an x-ray diffractometer with a Siemens Cu-anode x-ray tube.

The time evolution of the process was studied at 503 K, between 40 and 1620 min. The microstructure of samples was analyzed by transmission electron microscopy (TEM) (JEOL2000FX+EDS). The composition of the layer-structure and the interfaces were determined by an INA-X type SNMS (SPECS GmbH, Berlin) equipment which has extremely high lateral homogeneity and outstanding depth resolution ( $<2$  nm) at 300 eV  $\text{Ar}^+$  ion energy.<sup>9</sup> In this case the detection limit of the SNMS is about 10 ppm.<sup>8,9</sup>

SNMS intensity (cps)-sputtering time (s) curves of an as-deposited sample are shown in Fig. 1. The broad Ni/a-Si interface indicates the presence of a mixed  $\text{Ni}_x\text{Si}_{1-x}$  layer between the nickel and silicon. In obtaining the NiSi peak, which can be correlated with this mixed phase, the mass number of NiSi (58 amu+28 amu=86 amu) was measured. If nickel and silicon are present at a sputtered surface the formation of NiSi molecules might be expected as a consequence of ion bombardment. Thus, the presence of this phase could be an artifact of the method. However, the TEM investigation of the as-deposited Ni/a-Si sample confirms the presence of such reaction phase (inset in Fig. 1). The thickness of the mixed  $\text{Ni}_x\text{Si}_{1-x}$  layer is approximately 4 nm. Similar continuous and uniform initial nanometric layer was also detected by others<sup>10-12</sup> in this system.

The SNMS intensity versus sputtering time curves of an annealed sample (at 503 K for 1020 min) are presented in Fig. 2. The determination of the positions of the interfaces was carried out in subsequent steps. First the curves shown

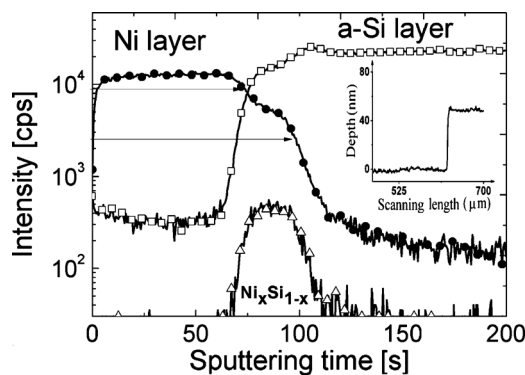


FIG. 2. Intensity-sputtering time spectra of the sample annealed at 503 K. The inset shows the profile of the crater (sputtered in the SNMS).

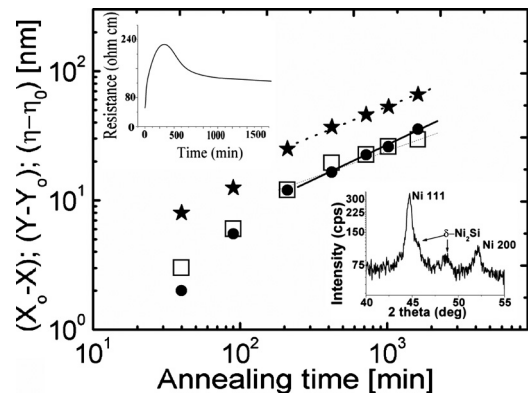


FIG. 3. Positions of the Ni/ $\text{Ni}_x\text{Si}_{1-x}$  and  $\text{Ni}_x\text{Si}_{1-x}$ /a-Si interfaces (□ and ●, respectively) and the average thickness of the product phase (×) vs the annealing time at 503 K on a  $\log_{10}$ - $\log_{10}$  plot. The insets (a) and (b) show the resistance vs annealing time function and the XRD spectra after 1620 min, respectively.

in Fig. 2 were determined and the intensity level of the inflexion points,  $I_{\text{inf}}$ , belonging to the drops in the curves were read out. Next profiling with the profilometer was carried out and the etching was followed until the value of  $I_{\text{inf}}$ , belonging to the interface in question, was reached and the depth was determined.

The arrows in Fig. 2 indicate the position where the sputtering process was finished and the depth of the obtained crater was measured. In determining the interface positions, in each case a new crater was created up to the given drop in the composition. The positions of the Ni/ $\text{Ni}_x\text{Si}_{1-x}$  as well as the  $\text{Ni}_x\text{Si}_{1-x}$ /a-Si interfaces, are denoted by X and Y, respectively. From the depth measurements the shrinkage of Ni ( $X_o - X$ ) and a-Si ( $Y - Y_o$ ) can be calculated. The initial positions  $X_o$  and  $Y_o$ , respectively, were determined on the as-deposited sample. In identifying the positions of the interfaces, up and down drops (half widths) of the NiSi signal were of help, too (Figs. 1 and 2). The  $Y - X = \eta$  gives the thickness of the  $\text{Ni}_x\text{Si}_{1-x}$  reaction phase. In Figs. 3 the shrinkage of the Ni and a-Si layers as well as the growth of the reaction phase are shown for different annealing times. It can be seen that these are monotonic functions of the annealing time. However, there is a break at about  $t \approx 200$  min on each of the above functions, indicating that there is a change in the kinetics of the shrinkage as well as growth processes. Obviously, e.g., if the kinetics would be a pure parabolic one the plots would result in single straight lines with a slope of 0.5.

In order to clear up the origin of the breakpoint mentioned above control electrical resistance measurements were carried out (insert in Fig. 3). At about 200 min the resistance falls down indicating the start of the crystallization process in the sample. XRD measurements were also performed on the sample annealed for 1620 min (second inset of Fig. 3). It can be seen that crystalline  $\delta\text{-Ni}_2\text{Si}$  phase is present. Between the two peaks of this phase pinches of one or two additional peaks can be observed, but the scatter of data is too high to get unequivocal conclusion whether this/these belong to  $\theta\text{-Ni}_2\text{Si}$  metastable phase or to NiSi phase (see, e.g., discussions in Refs. 13 and 14).

In order to get information about the composition of the phases formed one can transform (following Refs. 7 and 8) the intensity to concentration and the sputtering time to depth

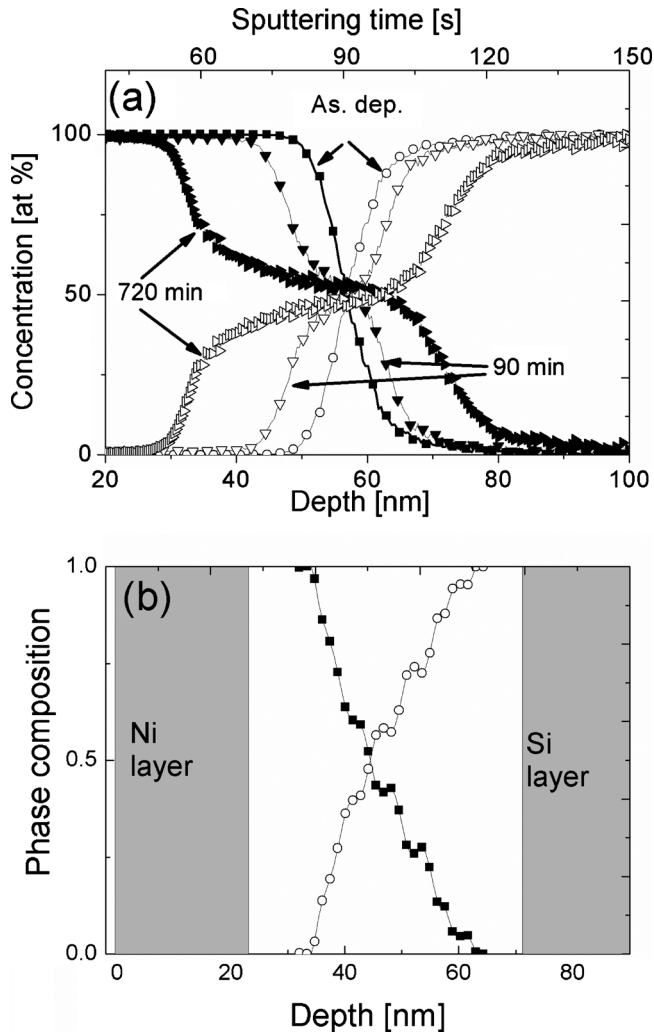


FIG. 4. (a) Composition-depth profiles of samples at different annealing times (full and open symbols show the Ni and Si concentrations, respectively). (b) Chemical phase profile of the transition region between the  $\text{Ni}_2\text{Si}$  and NiSi layers at 720 min (full and open symbols belong to  $\text{Ni}_2\text{Si}$  and NiSi, respectively).

from the SNMS intensity spectra as well as from the measured depth, respectively [Fig. 4(a)].

It can be seen in Fig. 4(a) that the product phase has a composition of about 50%–50% in the amorphous state (curve at 90 min), while at 720 min an additional shoulder can be observed at the composition of  $\text{Ni}_2\text{Si}$ . Thus, we can conclude that, in accordance e.g., with Ref. 1, up to about 200 min an amorphous NiSi phase grows with a rate different from the parabolic one (first part of the curves in Fig. 3). After this a partial crystallization of this phase into crystalline  $\text{Ni}_2\text{Si}$  phase(s) takes place and the average thickness of the reaction products increases by an approximately parabolic law (the value of the slopes of the second parts in Fig. 3 is about 0.5). The presence of the remaining amorphous reaction layer is also indicated by the fact that if all the consumed amount of Ni would be transformed into crystalline phase(s), the height of the corresponding XRD peaks should be comparable with the height of the (200) Ni peak.

In addition to Fig. 4(a), following the method described in Ref. 8, it is also possible to determine quantitatively the depth profiles of the  $\text{Ni}_2\text{Si}$  and NiSi phases being formed in the reaction region between the Ni and the Si layer. Such an evaluation has been made for the central part of the concentration depth profiles in Fig. 4(a) belonging to 720 min annealing time. The resulting depth dependent variation of the fractions of both phases is shown in Fig. 4(b).

Note that in solid state reactions between Ni and Si the type of the nickel-silicide phases formed depends on many factors such as the initial layer thicknesses and their ratio, the initial structure (amorphous or crystalline), deposition technique, annealing atmosphere, etc.<sup>1,2,14–16</sup> The detailed and more extended analysis of the types of the product phases and of the kinetics of the interface shifts is beyond the scope of this paper.

In conclusion a method has been demonstrated for the investigation of the interface shifts during solid state reaction in Ni/amorphous-Si systems. For the determination of the positions of the individual interfaces a combination of the SMNS technique and depth measurement by profilometer was applied. The kinetics of the shrinkage of the initial nanocrystalline Ni film and the amorphous Si layer as well as the average growth of the product phases were determined at 503 K. The results show that nanoscale resolution can be reached and the method is promising for following solid state reactions in different thin film systems.

The authors gratefully acknowledge the support of the Hungarian Scientific Research Fund (OTKA) through Grant Nos. CK 80126 and K 67969 and the bilateral Hungarian-Ukrainian TeT Project No. UA-4/2008. The work is also supported by TÁMOP 4.2.1-08/1-2008-003 project. Z. Erdélyi is a grantee of the “Bolyai János” scholarship.

<sup>1</sup>U. Gösele and K. N. Tu, *J. Appl. Phys.* **66**, 2619 (1989).

<sup>2</sup>F. Nemouchi, D. Mangelinck, C. Bergman, P. Gas, and U. Smith, *Appl. Phys. Lett.* **86**, 041903 (2005).

<sup>3</sup>B. E. Deal and A. Groves, *J. Appl. Phys.* **36**, 3770 (1965).

<sup>4</sup>F. d’Heurle, P. Gas, J. Philibert, and O. Thomas, *Met., Mater. Processes* **11**, 217 (1999).

<sup>5</sup>D. L. Beke and Z. Erdélyi, *Phys. Rev. B* **73**, 035426 (2006).

<sup>6</sup>C. Cserhádi, Z. Balogh, Gy. Glodán, A. Csik, G. A. Langer, Z. Erdélyi, G. L. Katona, D. L. Beke, I. Zizak, N. Darowski, E. Dudzik, and R. Feyerherm, *J. Appl. Phys.* **104**, 024311 (2008).

<sup>7</sup>H. Oechsner, in *The Physics of Ionized Gases*, edited by M. M. Popovic and P. Krstic (World Scientific, Singapore, 1985), p. 1403.

<sup>8</sup>H. Oechsner, R. Getto, and M. Kopnarski, *J. Appl. Phys.* **105**, 063523 (2009).

<sup>9</sup>K. H. Müller and H. Oechsner, *Mikrochim. Acta, Suppl.* **10**, 51 (1983).

<sup>10</sup>S. Oukassi, J. S. Moulet, S. Lay, and F. Hodaj, *Microelectron. Eng.* **86**, 397 (2009).

<sup>11</sup>N. Mattoso, *J. Mater. Sci.* **30**, 3242 (1995).

<sup>12</sup>L. A. Clevenger and C. V. Thomson, *J. Appl. Phys.* **67**, 1325 (1990).

<sup>13</sup>D. Mangelinck, K. Hoummada, and I. Blum, *Appl. Phys. Lett.* **95**, 181902 (2009).

<sup>14</sup>L. Ehouarne, M. Putero, D. Mangelinck, F. Nemouchi, T. Bigault, E. Ziegler, and R. Coppard, *Microelectron. Eng.* **83**, 2253 (2006).

<sup>15</sup>C. Lavoie, F. M. d’Heurle, C. Detavernier, and C. Cabral, *Microelectron. Eng.* **70**, 144 (2003).

<sup>16</sup>B. Bokhonov and M. Korchagin, *J. Alloys Compd.* **319**, 187 (2001).